CONF-750839--1

75-66

Note: This is a draft of a paper being submitted for publication. Contents of this paper should not be quoted nor referred to without permission of the authors.

BACKSCATTERING OF LIGHT IONS FROM METAL SURFACES

H. Verbeek

SOLID STATE DIVISION
OAK RIDGE NATIONAL LABORATORY
Operated by
UNION CARBIDE CORPORATION
for the
ENERGY RESEARCH AND DEVELOPMENT ADMINISTRATION
Oak Ridge, Tennessee

July 1975

BACKSCATTERING OF LIGHT IONS FROM METAL SURFACES*

H. Verbeek†
Solid State Division
Oak Ridge National Laboratory
Oak Ridge, Tennessee, 37830

ABSTRACT

When a metal target is bombarded with light ions some are implanted and some are reflected from the surface or backscattered from deeper layers. This results in an energy distribution of the backscattered particles which reaches from zero to almost the primary energy. The number of the backscattered particles and their energy, angular, and charge distributions depends largely on the energy and the ion target combination. For high energies (i.e. >50 keV for protons) particles are backscattered in a single collision governed by the Rutherford cross section. Protons and He-ions with energies of 100 keV to several MeV are widely used for thin film analysis. For lower energies multiple collisions and the screening of the Coulomb potential have to be taken into account, which makes the theoretical treatment more difficult. This energy region is, however, of special interest in the field of nuclear fusion research. Some recent results for energies below 20 keV are discussed in some detail.

---

*Research sponsored by the U. S. Energy Research and Development Administration under contract with the Union Carbide Corporation.

†Guest Scientist from the Max Planck Institut für Plasmaphysik, D-8046 Garching, West Germany.

INTRODUCTION

When a beam of ions impinges onto a metal target, some of the ions are implanted and some are reflected from the surface or backscattered from deeper layers. The implanted atoms may diffuse to the surface and be released with thermal energies or they may be trapped inside the material, e.g. at lattice defects. They also may cluster together and form gas bubbles inside the metal. The amount of trapping depends strongly on the particular ion target combination, on the temperature, and on the bombardment dose. This paper deals only with the particles which are kinetically backscattered, and is restricted to light ions such as hydrogen and helium.

The particles which are backscattered give rise to an energy distribution which extends from zero energy to almost the primary energy. A typical example is given in Fig. 1, which shows the energy distribution for 15 keV protons backscattered from an Au target. The sharp threshold at high energies is due to ions which are backscattered from the surface atoms of the target. The position of this edge is determined by the kinematics of a single scattering event. When a particle of mass M_1 and an energy E_1 is scattered from an atom with mass M_2 the energy after scattering is

$$E_2 = k^2 E_1$$

where $$k = [M_1 \cos\Theta + (M_2^2 - M_1^2 \sin^2\Theta)^{\frac{1}{2}}]/(M_1 + M_2) \qquad (1)$$

for $M_1 < M_2$ and Θ is the scattering angle in the laboratory system.

The backscattering intensity in Fig. 1 at lower energies results from scattering events deeper in the solid. Along their passage through the solid the particles lose energy in elastic nuclear collisions and quasi-continuously by excitation of target electrons[1,2]. Therefore, they

appear outside the target with all energies below the energy of the particles backscattered from the surface.

This paper is divided into three sections, with each treating a certain range of primary energies. As will be shown these energy ranges arise quite naturally from the different theoretical and experimental treatments of the backscattering effect they require.

For protons at energies above ≈ 50 keV the scattering can be well described by the single collision model[3,4,5]. This model assumes that the backscattering occurs in a single large angle deflection from a certain nuclear collision, which is describable by the Rutherford cross section[6]. The trajectories of the ions inside the material to the scattering center and back to the surface are taken as straight lines. Along their trajectories they lose energy by excitation of the target electrons. This can be described by the differential energy loss dE/dx, i.e. the energy loss per unit path length. This makes the theoretical calculation of the energy spectra rather simple.

For this energy range the most convenient measuring method utilizes surface barrier detectors. These give energy proportional signals which are easily analyzed in a multi-channel analyzer system. They are equally sensitive to ions and neutral atoms.

At high energies, depending strongly on the ion target combination, the validity of the Rutherford scattering law is limited by the occurrence of nuclear reactions and resonances. This area will be covered by R. S. Blewer, this conference. A compilation of nuclear reaction data may be found in Refs. 7 and 8.

Protons and helium ions which are easily available from small accelerators with energies from ≈ 100 keV to several MeV are widely used for surface layer analysis and depth profiling[9].

At energies below ≈ 50 keV the screening of the nuclear charge by the outer electrons becomes more important. Thus the Coulomb potential leading to the Rutherford cross section is no longer appropriate. More complicated potentials which are derived from the Thomas–Fermi theory have to be used[2]. Also the validity of the single collision model breaks down. With decreasing energy the cross section for nuclear collisions increases and one has to account for multiple collisions of the backscattered particles. The theoretical treatment becomes much more complicated. An analytical form for the energy distributions can no longer be derived.

Also the experimental techniques must be modified. At energies below ≈ 20 keV surface barrier detectors are no longer suitable to give energy information. Electrostatic or magnetic energy analyzers can be used, but these are only sensitive to charged particles. Also, the charged fraction of the backscattered particles decreases with decreasing energy[10,11,12] and the spectra of the neutral and charged components may be very different[11]. Thus one needs a means to ionize the neutral backscattered particles in a definite manner, if quantitative results are to be obtained. Another method to overcome this difficulty is to use time of flight techniques[13], but these too require particle detectors with known sensitivity for neutrals.

The range of primary energies 5 to 20 keV is of special interest for fusion technology. For plasma experiments and later fusion reactors where

the mean particle confinement times in the plasma are much shorter than the desired burning times, an important role is played by the interaction of the diffusing plasma particles with the first walls. Particularly with respect to the question of recycling[14], it is important to know the total number and angular, energy, and charge distributions of light ions (H, D, T, He) backscattered from solid surfaces.

Below the primary energy of ≈ 1 keV the experiments are extremely difficult. Most of the backscattered particles are neutral and the ionization and detection methods currently in use break down at these low energies. To my knowledge there are no experiments in this energy range dealing with the total number of backscattered particles. Consequently, one has to rely on computer simulations. The backscattering of primary ions with energies below 1 keV are of particular interest for today's plasma experiments.

If one investigates the backscattering from single crystals the results are largely influenced by the crystal structure which gives rise to channeling and blocking effects. This offers a large variety of measuring methods in depth profiling and lattice site determining. Recent reviews are given in Refs. (15) and (16); the present review deals only with the backscattering from amprphous or polycrystalline materials.

HIGH ENERGIES

The principle of backscattering of ions with primary energies larger than ≈ 50 keV can be explained with the aid of Fig. 2. A particle of Energy E_1 enters a solid at an angle α to the surface normal. The trajectory inside the solid is a straight line until it encounters a target atom at a distance close enough to cause a large angle deflection. The

outgoing ion trajectory is again taken as a straight line and it leaves the surface at an angle β to the normal. (In the experiment α and β are determined by the primary beam direction and the position of the detector with respect to the target.)

Along their paths through the solid the particles lose energy. For light ions with energies above a few keV the energy loss is primarily due to ionization and excitation of target electrons[17]. One can describe that by the differential energy loss dE/dx measured in eV/Å or MeV/(mg/cm^2). Sometimes it is more convenient to use the stopping cross section or stopping power $\varepsilon = 1/N\ dE/dx = M_2/(N_o \rho)\ dE/dx$, where N is the number of target atoms per unit volume, N_o Avogadro's number, ρ the density and M_2 the mass number of the target atoms. Thus ε is measured in eV cm^2/atom. dE/dx (or ε) is a function of energy. Today a number of stopping power tables are available (18, 19, 20). These are semiempirical tables based on experimental data which are inter- and extrapolated using theoretical functional dependences. As an example, Fig. 3 shows dE/dx curves for H^+ and He^+ in Ni from the tables of Northcliffe and Schilling[19]. A review on the various energy loss mechanisms has recently been given by Sigmund[21].

With the scheme of Fig. 2 the energy of the outcoming particles E_2 can be related to the depth from which the backscattering occurs. Particles which are backscattered from the surface have lost energy only in the elastic collision, i.e. $E_2 = k^2 E_1$ according to formula (1). For regions not too far from the surface the relation between depth x and the observed energy E_2 is:

$$\Delta E = k^2 E_1 - E_2(x) = \left(\frac{k^2}{\cos \alpha} \left(\frac{dE}{dx}\right)_{\bar{E}_1} + \frac{1}{\cos \beta} \left(\frac{dE}{dx}\right)_{\bar{E}_2}\right) x \qquad (2)$$

ΔE is the difference between the energies of particles backscattered from the surface and from a depth x, $(dE/dx)_{\bar{E}_1}$ and $(dE/dx)_{\bar{E}_2}$ are the differential energy losses for the mean energies along incoming and outcoming trajectories. For this formula it was assumed that dE/dx varies only slightly along the trajectories of the particles. For the analysis of thick layers the target can be divided into thin slices. For each slice the incident energy can be calculated using the dE/dx curve. In many laboratories, computer programs are used for this procedure.

When composite targets--compounds or mixtures--are investigated, one obtains an overlay of the spectra of each component. These are shifted in energy relative to each other due to the dependence of k^2 on the target atom mass number M_2 (Formula 1). The stopping power for a compound is the sum of the stopping powers of the constituents weighted by the relative amounts with which they occur in the compound (Bragg's rule[22]). This relation has been proved valid in a number of cases[23]. For instance, the stopping power in SiO_2 is $\varepsilon_{SiO_2} = \varepsilon_{Si} + 2\varepsilon_O$. A rigorous treatment of the analysis of targets whose composition varies with depth was given by Brice[24].

An example of these principles is presented in Fig. 4, which shows the spectrum of 2 MeV He^+ ions backscattered from a film of Nb_3Ge (a compound with high superconducting T_c) deposited on an Al_2O_3 substrate[25]. The spectra of the constituents of the film and of the substrate are clearly visible. The structure on top of the backscattering spectrum indicates that this film is not uniform. It is Ge rich near the surface. At the

high energy edge the slope of the spectrum is determined by the detector resolution. At the interface between film and substrate the slope is considerably less steep. This is due to straggling in the energy loss. Energy straggling becomes increasingly important with increasing depth, and it finally limits the resolution of backscattering spectrometry. Energy straggling depends on the energy and on the ion-target combinations. It was treated theoretically in an early paper by Bohr[1] and by Lindhard et. al.[17]. For an example of recent experimental determinations using backscattering techniques, see Ref. 26.

The backscattering yield, i.e. the height H of the energy distributions (number of counts per channel) is related to the number density of atoms in a layer dx near the surface:

$$H = Q\sigma\Omega N dx \tag{3}$$

where Q is the number of primary particles arriving on the target, Ω the solid angle subtended by the detector, N the number of target atoms per unit volume, and σ the cross section averaged over the solid angle $[\sigma = 1/\Omega \int (d\sigma/d\Omega) d\Omega]$. It has been shown[5] that for protons with energies >50 keV the Rutherford cross section is valid. In laboratory coordinates this is[27]:

$$d\sigma = \frac{Z_1 Z_2 e^2}{16E} \cdot f(\Theta) d\Omega$$

$$f(\Theta) = 4[\cos\Theta + \{1-(\tfrac{M_1}{M_2}\sin\Theta)^2\}^{\frac{1}{2}}] \sin^{-4}\Theta \{1-(\tfrac{M_1}{M_2}\sin\Theta)^2\}^{\frac{1}{2}} \tag{4}$$

where Z_1, Z_2 and M_1, M_2 are the nuclear charges and mass numbers of projectiles and target atoms, e the elementary charge, and Θ the scattering angle. Using Formula (2), dx in Formula (3) can easily be related to an energy interval dE_2 (for instance that corresponding to the width of a channel in the multichannel analyzer), when it is assumed that dE/dx is

constant for the energy interval under consideration. If the functional energy dependence of the stopping cross section from energy is known, formulae for the backscattering yield from thick targets can be derived[28,29]. With these the stopping cross sections can be determined from the absolute height of the energy distributions[28,30,31].

If the particles are backscattered from a thin film of thickness t, the sum of the counts in all channels containing counts due to particles backscattered from this film is:

$$\int H(E_2)dE_2 = Q\sigma\Omega Nt \qquad (5)$$

This is independent of the stopping power. Thus the number of target atoms per unit area, Nt, can be determined directly.

As an example in Fig. 5 the backscattering of 150 keV protons from a Nb film on a Be substrate is shown[32]. This film was sputtered by 5 keV deuterons. From the decrease of the number of backscattered particles after sputtering the sputtering yield could be determined.

Backscattering is a very unlikely process in this energy range. To illustrate this let us assume a 1 μm thick Ni foil which is bombarded by 1 MeV protons. A detector of 1 cm diameter in a distance of 10 cm from the target at $\Theta = 135°$ counts only 1.1×10^{-7} particles per incident ion. Nevertheless this is a very useful and nondestructive method for surface analysis. In some cases surface impurities of less than 10^{-4} monolayers have been detected[33].

MEDIUM ENERGIES

As mentioned already in the introduction, surface barrier detectors are no longer suitable to measure particle energies below 20 keV. It is

straightforward in this energy range to use electrostatic or magnetic spectrometers. These are, naturally, only sensitive to charged particles. There are several papers[4, 34-37] which report on measured energy distributions of the charged component of the backscattered particles. Most of the backscattered particles are, however, neutral at energies below 40 keV (for hydrogen)[10,11,12]. A comparison with the theoretical values is only possible if the total number of backscattered particles is known since the theory of the charged fraction is not yet well developed. Therefore, a direct measurement of the neutrals seemed to be desirable. Buck et. al.[13] successfully performed time of flight measurements for He in the energy range of 6 to 32 keV.

Another method, which we have used at the IPP in Garching, is to ionize the neutral particles by stripping in a gas cell[10,11]. The principle is explained by Fig. 6. A magnetically selected ion beam impinged onto the target, which could be rotated such that the entrance and exit angles α and β could be varied. A scattered beam intensity corresponding to a scattering angle of $\Theta = 135°$ was selected. With deflection plates the charged component could be removed from the beam. In the stripping cell, which was filled with 2×10^{-3} Torr N_2, a part (known from a previous calibration) of the neutrals was ionized and energy analyzed in a 90° electrostatic spectrometer which utilized a channeltron multiplier detector.

Representative measurements of the energy distributions of positively charged and neutral particles backscattered at $\Theta = 135°$ from a Ta target bombarded with 18.5 keV protons are shown in Fig. 7. The charged fraction $Q = N^+/N^+ + N^\circ$, i.e. the number of positively charged to the number of

neutrals plus positives, decreases from ≃ 40% at 20 keV to ≃ 10% at 2 keV. Both the neutral and the charged spectra show distinct maxima at low energies. It is also seen that besides their relative height, the shapes of the two spectra are rather different. Consequently, a derivation of the neutral spectrum from the charged is not easily accomplished. The shapes of the backscattering spectra depend only slightly on the target material. For decreasing primary energy the maximum is more pronounced, but the charged fraction depends only on the exit energy. The charged fraction decreases slightly with increasing angle of emergence β[11]. At low energies negative particles were also observed[38]. In this case the negative fraction is small, but especially with target materials with low work function, the negative fraction may be much larger than the positive.

In a separate experiment an electrostatic analyzer was used, which could be swivelled around the target in order to determine the angular distribution of the particles backscattered when a proton beam is impinging normal onto a Nb target[39]. With this instrumentation only the charged component (including positive and negative ions) could be measured. For protons on Nb it was possible to determine the total number of backscattered particles using the charged fraction measured previously (11).

It is shown in Ref. 39 that the angular distribution of all backscattered particles is very close to a cosine distribution for primary proton energies from 4 to 15 keV. Only the ions scattered with the highest energies are preferrential scattered into smaller scattering angles. These contribute, however, only very little to the total back-

scattering intensity. Two examples of energy distributions of all particles backscattered into the whole half-space are shown in Fig. 8. Both spectra with primary energies E_1 = 10.22 keV and E_1 = 4.16 keV (measured with 8.32 keV H_2+ ions) show a distinct maximum at ≈ 1 keV. This is due to the fact that the scattering cross section increases as the ions lose energy in the solid. Below the maximum the probability of multiple scattering and removal from the beam exceeds the probability of backscattering events. By integration of the spectra in Fig. 8 over all energies the reflection coefficient R, i.e. the number of backscattered to incoming particles, can be determined. In Fig. 9 our results on the backscattering coefficients are shown together with theoretical and experimental values from other authors. R increases rapidly as the primary energy is lowered.

In the theoretical work of Weissmann and Sigmund[40] and of Böttiger and Winterbon[41] the slowing down of the protons in an amorphous solid of infinite extent is calculated by means of the Boltzmann transport equation. This model assumes that the atoms start from a plane in the solid. All atoms which finally come to rest behind this plane are considered to be backscattered. Böttiger and Winterbon[41] also include a surface correction. The values of J. E. Robinson[42], O. S. Oen and M. T. Robinson[43] as well as the value for Mo by Ishitani, et. al.[44] were obtained by computer simulation. These simulations also assume amorphous materials.

The fact that the experimental results are considerably lower than those from the calculations can probably be attributed to two main differences: (1) the Nb target had rather large crystal grains. Thus the backscattering was more from individual single crystals than from amor-

phous material. This leads to larger penetration depths and hence less backscattering. For $E_1 \approx 10$ keV, Oen[43] also simulated a polycrystalline target and obtained a backscattering coefficient, which is much smaller than the value for amorphous material. (2) The Nb was very likely covered with an oxide layer which also reduces the backscattering.

In Fig. 9 recent experimental results of Sidenius[45] measured on Au are included. (To compare the values for Au with those for Nb they were plotted at reduced energies[17] $\varepsilon = E \cdot a\, M_2/[(M_1+M_2)Z_1Z_2e^2]$, where $a = 0.468\ (Z_1^{\frac{2}{3}} + Z_2^{\frac{2}{3}})^{-\frac{1}{2}}$ Å is the screening length of the interaction potential.) Sidenius had his target mounted inside a proportional counter so that all the backscattered particles were absorbed and created pulses proportional to their energy. These results are close to the theoretical values. An oxide layer cannot be expected in the case of Au, which indicates again the influence of such a layer on our results.

Recently Bøttiger and Rud[46] determined the trapping coefficient of He^3 in Au using a nuclear reaction. When no gas is released thermally, the sum of the trapping and reflection coefficients is unity. The values obtained by this method are also in good agreement with theory.

The knowledge of reflection coefficients as well as energy and angular distributions is very important for plasma experiments. Therefore, more experiments are necessary. Another important number in this context is the energy reflection coefficient γ, i.e. the total energy carried away by the backscattered particles related to the incoming energy. It is $\gamma = R\bar{E}/E_1$, where $\bar{E}$ is the mean energy of all reflected particles. $\bar{E}$ can be determined from the spectra as in Fig. 8. The energy reflection coefficient γ was recently directly measured by a Danish group[47] using

different calorimetic methods. They find good agreement with the computer simulation of O. S. Oen and M. T. Robinson[43].

LOW ENERGIES

At very low energies the fraction of the backscattered particles which are charged becomes very small. At energies below ≈ 200 eV, the ionization method by stripping in a gas cell breaks down and because the cross sections for electron loss are small compared to those for scattering in the gas and the latter effect distorts energy and angular distributions. In the energy range above several tens of eV the ionization by electron impact is also impossible since the required electron densities cannot be achieved. The detection methods for neutrals also break down. All currently used methods for detecting neutrals depend on the creation of secondary electrons. At energies where the potential emission of ions dominates the kinetic emission ($\lesssim$ 200 eV) there is no longer any emission of secondary electrons by neutrals. Because of the lack of detectors also the time of flight methods are then no longer usable at these low energies.

Therefore, one has to rely on the results of computer simulations. These are, in turn, especially suitable for low energies since it is easy to obtain sufficient statistics without too much computer time. Energy and angular distributions for protons scattered from Cu obtained recently by O. S. Oen and M. T. Robinson[43] are shown in Fig. 10. The energy distribution with a primary energy of 5 keV shows a maximum at ≈ 1 keV which agrees with the experimental observations. At a primary energy of 100 eV the spectrum is sharply peaked at high energies corresponding to

backscattering from the surface. The angular distributions show remarkable deviations from a cosine distribution, which would give the dotted lines. The backscattered intensity is peaked in the entrance direction which was normal to the surface. At grazing incidence the authors found reflection coefficients close to 1 with the intensity highly peaked in the direction of specular reflectance.

ACKNOWLEDGMENTS

I am indebted to B. R. Appleton, J. W. Miller, O. S. Oen, M. T. Robinson, H. H. Anderson, and J. Bøttiger for making their results available to me prior to publication. I appreciate a critical reading of the manuscript by B. R. Appleton and O. S. Oen. Finally I want to thank the people of the Solid State Division of ORNL for their warm hospitality I experienced during my year in Oak Ridge.

REFERENCES

1. N. Bohr, Kgl. Dan. Vid. Selsk. Mat. Fys. Medd. 18, No. 8 (1948).
2. J. Lindhard, V. Nielsen and M. Scharff, Kgl. Dan. Vid. Selsk. Mat. Fys. Medd. 36, No. 10 (1968).
3. S. Rubin, Nucl. Inst. Meth. 5, 177 (1959).
4. G. H. McCracken and N. J. Freeman, J. Phys. B 2, 661 (1969).
5. A. van Wijngaarden, E. J. Brimmer and W. E. Baylis, Can. J. Phys. 48, 1835 (1970).
6. E. Rutherford, Phil. Mag. 21, 669 (1911).
7. W. F. Hornyak, T. Lauritzen, P. Morrison and W. A. Fowler, Revs. Mod. Phys. 22, 291 (1950).
8. F. K. McGowan, W. T. Milner, H. J. Kim and Wanda Hyatt, Nuclear Data Tables 6, 353 (1969); 7, 1 (1969).
9. See for instance: "Ion Beam Surface Layer Analysis" ed. by J. W. Meyer and J. F. Ziegler, Elsevier Sequoia, Lausanne (1974).
10. R. Behrisch, W. Eckstein, P. Meischner, B.M.U. Scherzer and H. Verbeek, Atomic Collisions in Solids, ed. by S. Datz, B. R. Appleton, and C. D. Moak, Plenum Press, N.Y. 315 (1975).
11. P. Meischner and H. Verbeek, J. Nucl, Mat. 53, 276 (1974) and Report IPP, 9/18 (1975).
12. T. M. Buck, L. C. Feldman and G. H. Wheatley, Atomic Collisions in Solids, ed. by S. Datz, B. R. Appleton and C. D. Moak, Plenum Press, N.Y. 331 (1975).

13. T. M. Buck, Y. S. Chen, G. H. Wheatley and W. F. van der Weg, *Surface Science* 47, 244-255 (1975).

14. E. Hinnov, J. Nucl. Mat. 53, 9 (1974).

15. D. S. Gemmell, Revs. Mod. Phys. 46, 129 (1974).

16. D. V. Morgan (ed.),"Channeling, Theory, Observation and Applications", Wiley, N.Y. (1973).

17. J. Lindhard, M. Scharff and H. E. Schiøtt, Kgl. Dan. Vid. Selsk. Mat. Fys. Medd. 33, No. 14 (1963).

18. W. Whaling, "Encyclopedia of Physics", ed. by S. Flügge, Springer Verl. 34, 193 (1958).

19. L. C. Northcliffe and R. F. Schilling, Nucl. Data Tables A 7, 233 (1970).

20. J. F. Ziegler and W. K. Chu, Atomic Data and Nucl. Data Tables 13, No. 5 (1974).

21. P. Sigmund, Proceedings of the Advanced Study Institute on Radiation Damage Processes in Materials, Corsica (1973).

22. W. H. Bragg and R. Kleeman, Phil. Mag. 10, S 318 (1905).

23. J. S.-Y. Feng, W. K. Chu and M.-A. Nicolet, Thin Solid Films 19, 227 (1973).

24. D. K. Brice, Thin Solid Films 19, 121-135 (1973).

25. J. W. Miller, B. R. Appleton and J. R. Gavaler to be presented at the International Conference on Ion Beam Surface Layer Analysis, Karlsruhe, Sept. 15-19 (1975).

26. J. M. Harris, W. K. Chu and M.-A. Nicolet, Thin Solid Films 19, 259 (1973).

27. For a derivation of this formula, see J. F. Ziegler and R. F. Lever, Thin Solid Films 19, 291 (1973).

28. R. Behrisch and B. M. U. Scherzer, Thin Solid Films 19, 247 (1973).

29. W. K. Chu and J. F. Ziegler, J. Appl. Phys. 46, 2768 (1975).

30. W. A. Wenzel and W. Whaling, Phys. Rev. 87, 499 (1952).

31. D. Powers and W. Whaling, Phys. Rev. 126, 61 (1962).

32. W. Eckstein, B. M. U. Scherzer and H. Verbeek, Rad. Effects 18, 135 (1973).

33. J. D. Ball, T. M. Buck, C. W. Caldwell, D. McNair and G. H. Wheatley, Surf. Sci. 30, 69 (1972).

34. E. R. Cawthron, D. L. Cotterel and M. Oliphant, Proc. Roy. Soc. Lond. A319, 435 (1970).

35. K. Morita, H. Akimune and T. Suita, Jap. J. Appl. Phys. 7, 916 (1968).

36. W. Eckstein and H. Verbeek, J. Vac. Sci. Technol. 9, 612 (1972).

37. E. S. Mashkova and V. A. Molchanov, Rad. Effects 13, 131 (1972).

38. H. Verbeek, W. Eckstein and S. Datz, to be published.

39. H. Verbeek, J. Appl. Phys. 46, 2981 (1975).

40. R. Weissmann and P. Sigmund, Rad. Effects 19, 7 (1973).

41. J. Bøttiger and K. B. Winterbon, Rad. Effects 20, 65 (1973).

42. J. E. Robinson, Rad. Effects 23, 29 (1974).

43. O. S. Oen and M. T. Robinson, to be presented at the 6th International Conference on Atomic Collisions in Solids, Amsterdam, Sept. 22-26 (1975).

44. T. Ishitani, R. Shimizu and K. Murata, Jap. J. Appl. Phys. 11, 125 (1972).

5. G. Sidenius, Phys. Lett. A 49, 409 (1974).

6. J. Bøttiger and N. Rud, to be presented at the International Conference on the Application of Ion Beams to Materials, September 8-12, 1975, Warwick, England.

7. H. H. Anderson, T. Lenskjaer, G. Sidenius and H. Sørensen, to be published in J. Appl. Phys.

FIGURE CAPTIONS

Fig. 1. Energy distribution of hydrogen atoms backscattered from Au which is bombarded by 15 keV protons.

Fig. 2. Principle of the backscattering of light ions from a solid.

Fig. 3. Differential energy loss for H and He ions in Ni from Ref. 19.

Fig. 4. Backscattering spectrum of 2 MeV He from a Nb_3Ge film on an Al_2O_3 substrate[25].

Fig. 5. Energy distributions of protons backscattered at an angle of $\Theta = 135°$ from a 600 Å Nb film on a Be substrate before and after sputtering with 5 keV D^+ ions[32].

Fig. 6. Experimental setup for the detection of neutral backscattered particles.

Fig. 7. Energy distributions of neutral and positively charged hydrogen atoms backscattered from Ta bombarded with 18.5 keV protons. The charged fraction $N^+/N^+ + N^0$ is given by dots.

Fig. 8. Energy distributions of all particles backscattered into 2π solid angle when a Nb target is bombarded with 10.22 keV H_1^+ and 8.32 keV H_2^+ ions.

Fig. 9. Experimental and theoretical reflection coefficients for hydrogen as a function of the primary energy.

Fig. 10. Energy (left) and angular (right) distrubutions of hydrogen atoms backscattered from Cu bombarded with 100 eV and 5000 eV protons. (Computer simulation by Oen and Robinson[43].)

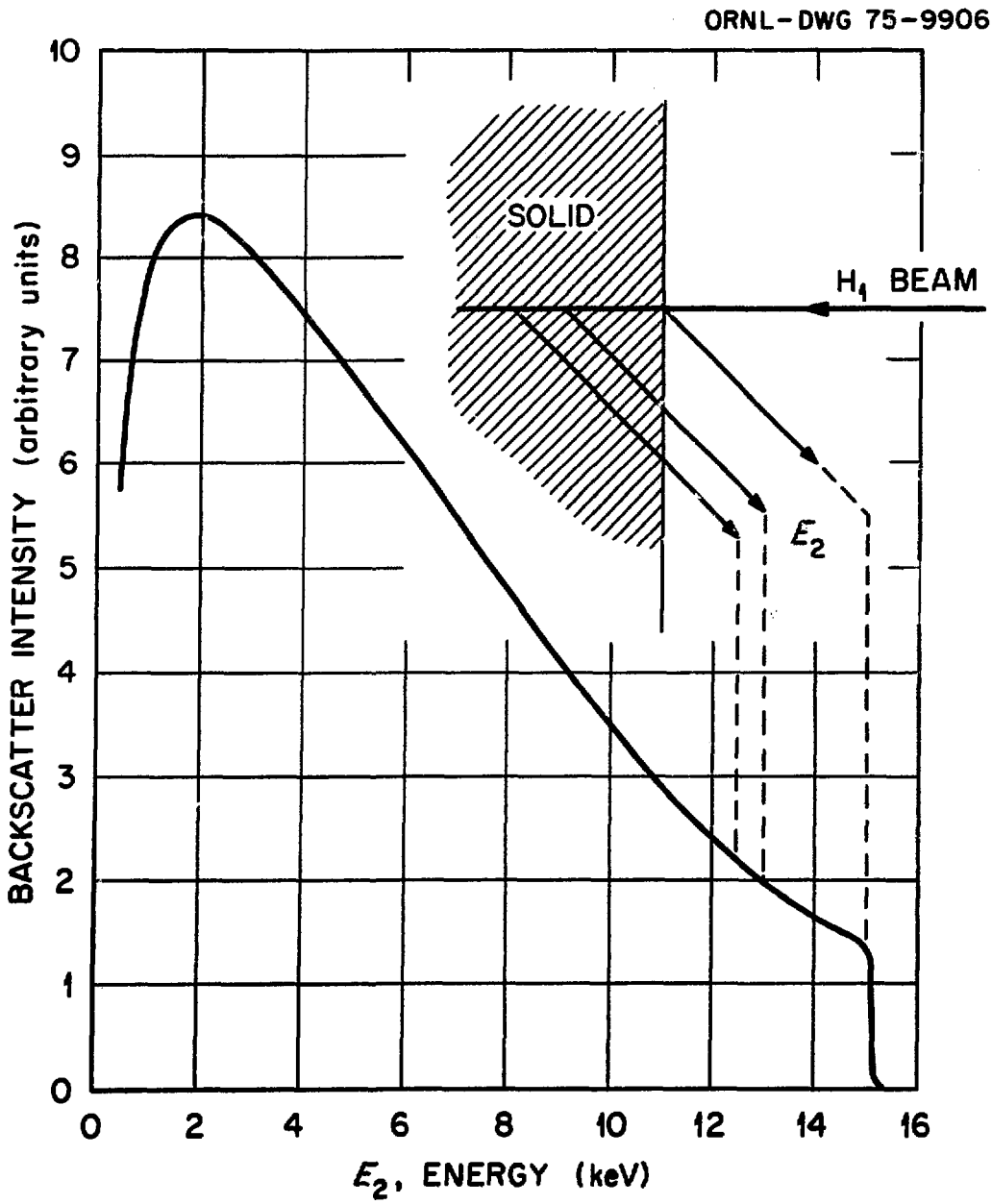
ORNL-DWG 75-9906
SOLID
H_1 BEAM
E_2
BACKSCATTER INTENSITY (arbitrary units)
E_2, ENERGY (keV)
0
1
2
3
4
5
6
7
8
9
10
0
2
4
6
8
10
12
14
16

Fig. 1

ORNL-DWG 75-9905

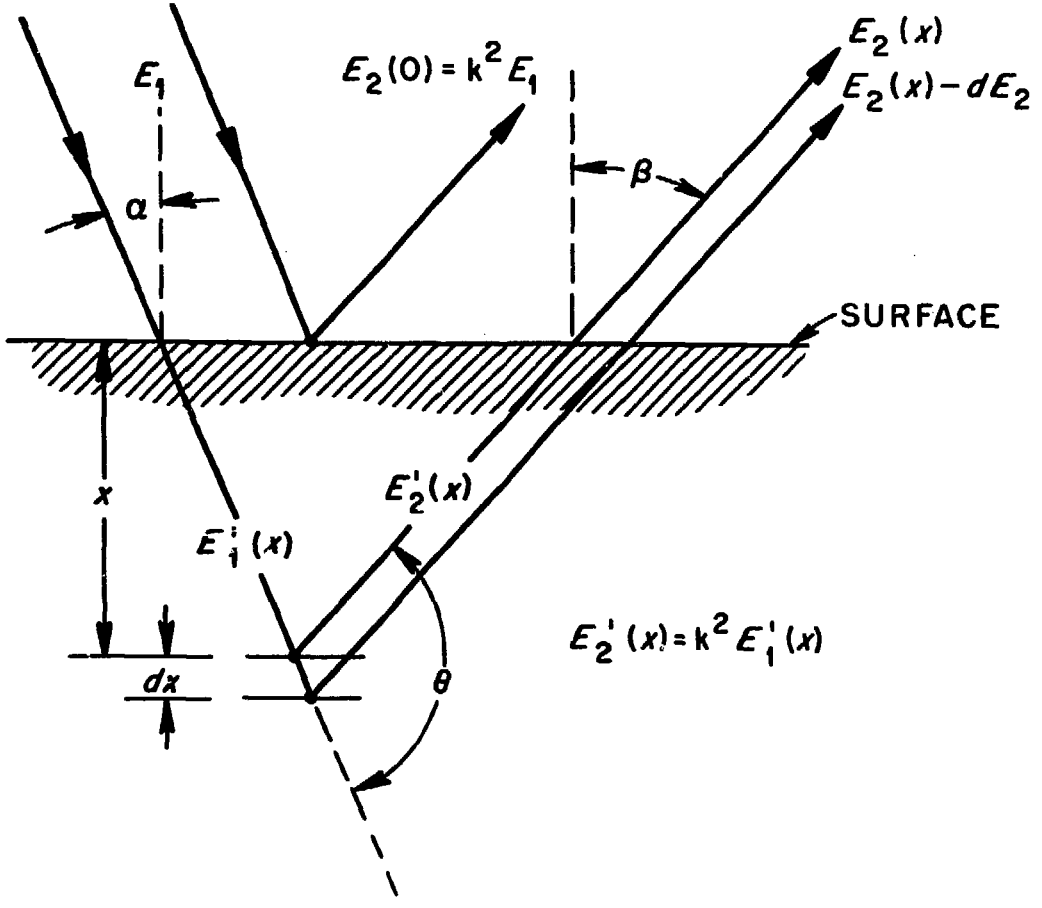

Fig. 2

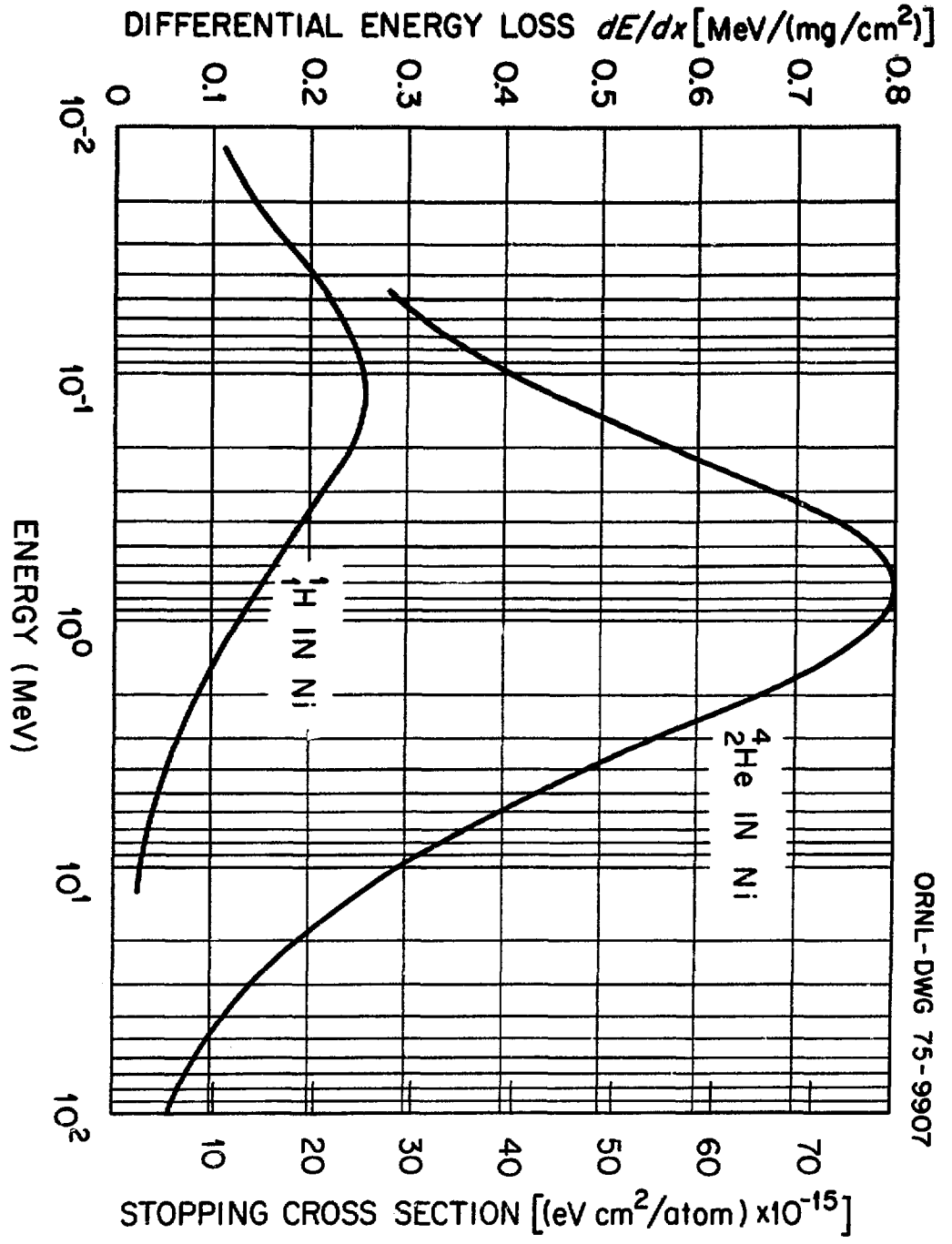
DIFFERENTIAL ENERGY LOSS dE/dx [MeV/(mg/cm²)]
0
0.1
0.2
0.3
0.4
0.5
0.6
0.7
0.8
ENERGY (MeV)
10⁻²
10⁻¹
10⁰
10¹
10²
¹₁H IN Ni
⁴₂He IN Ni
ORNL-DWG 75-9907
10
20
30
40
50
60
70
STOPPING CROSS SECTION [(eV cm²/atom) x10⁻¹⁵]

Fig. 3

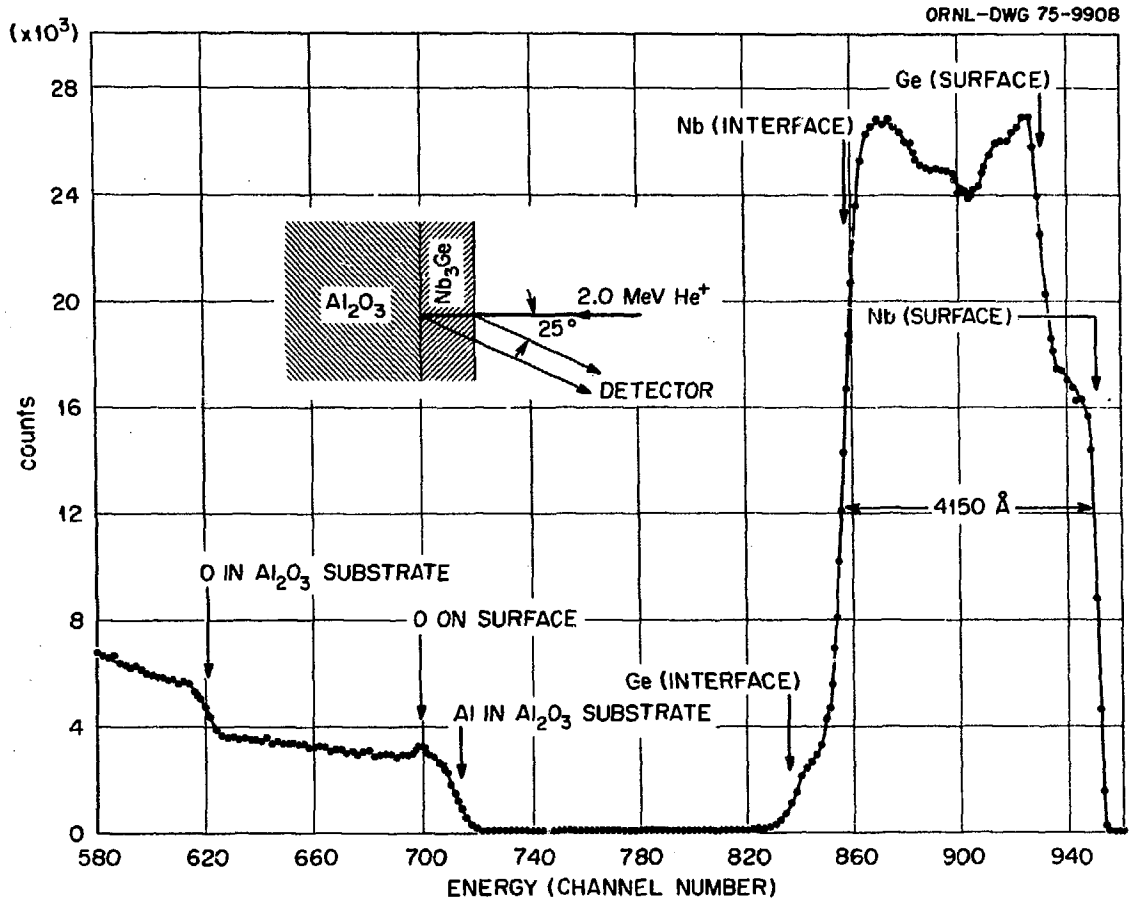
ORNL-DWG 75-9908
(x10³)
28
24
20
16
12
8
4
0
counts
Ge (SURFACE)
Nb (INTERFACE)
Nb (SURFACE)
4150 Å
Al2O3
Nb3Ge
2.0 MeV He+
25°
DETECTOR
O IN Al2O3 SUBSTRATE
O ON SURFACE
Ge (INTERFACE)
Al IN Al2O3 SUBSTRATE
580
620
660
700
740
780
820
860
900
940
ENERGY (CHANNEL NUMBER)

Fig. 4

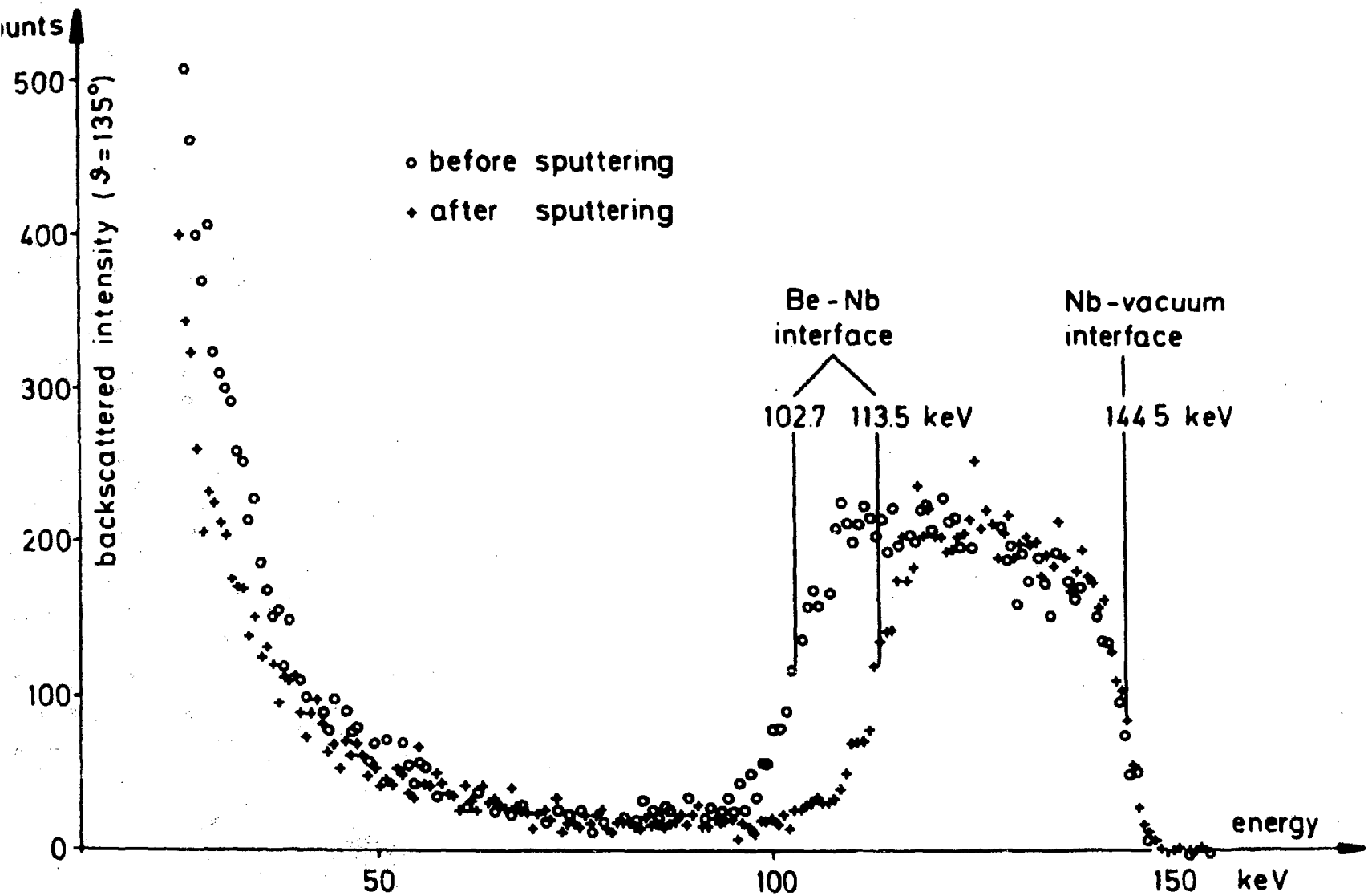
unts
500
400
300
200
100
0
backscattered intensity (ϑ=135°)
o before sputtering
+ after sputtering
Be - Nb
interface
102.7
113.5 keV
Nb - vacuum
interface
144.5 keV
energy
50
100
150
keV

Fig. 5

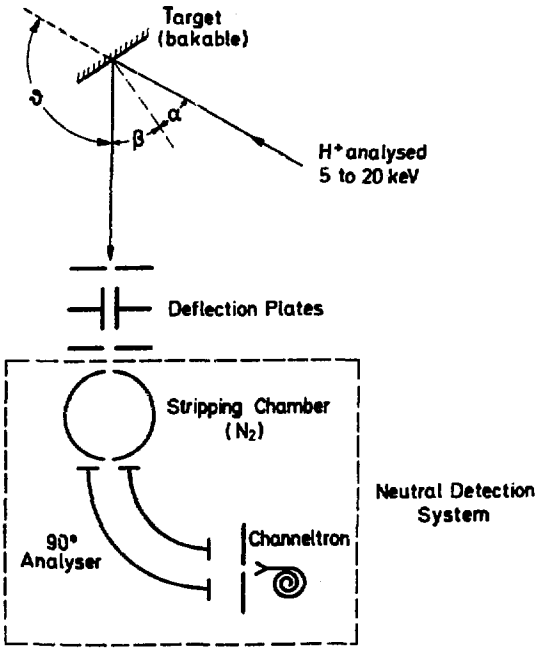
Target
(bakable)
ϑ
α
β
H⁺ analysed
5 to 20 keV
Deflection Plates
Stripping Chamber
(N2)
Neutral Detection
System
90°
Analyser
Channeltron

Fig. 6

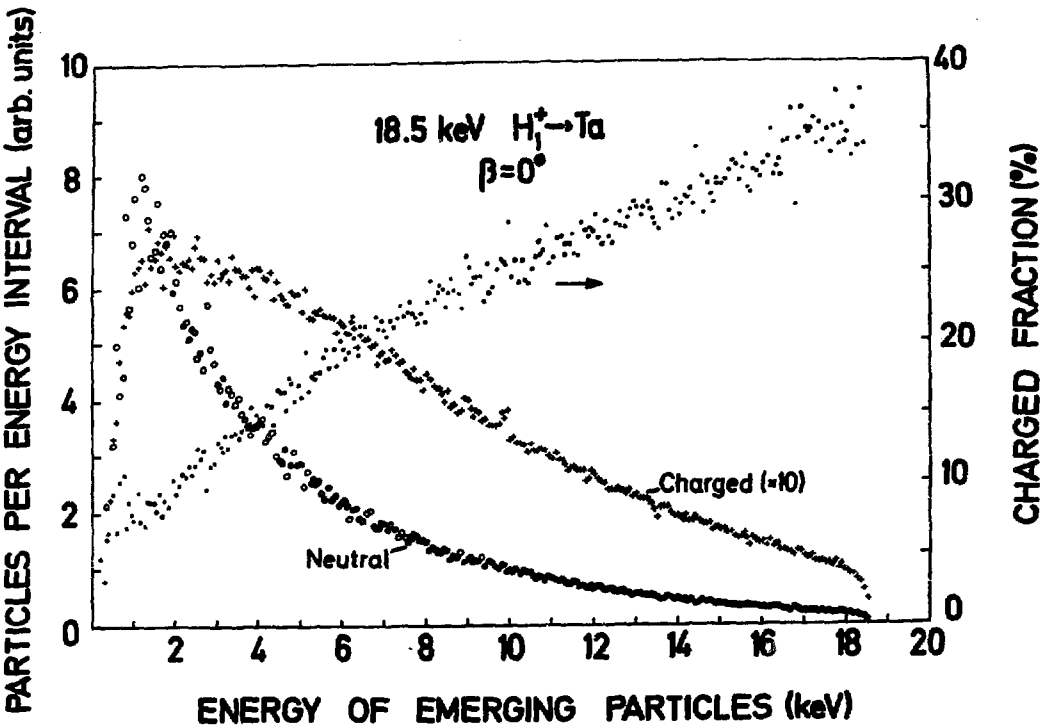
18.5 keV $H_1^+ \rightarrow Ta$
$\beta = 0°$
Charged (×10)
Neutral
PARTICLES PER ENERGY INTERVAL (arb. units)
CHARGED FRACTION (%)
ENERGY OF EMERGING PARTICLES (keV)
0
2
4
6
8
10
12
14
16
18
20
30
40

Fig. 7

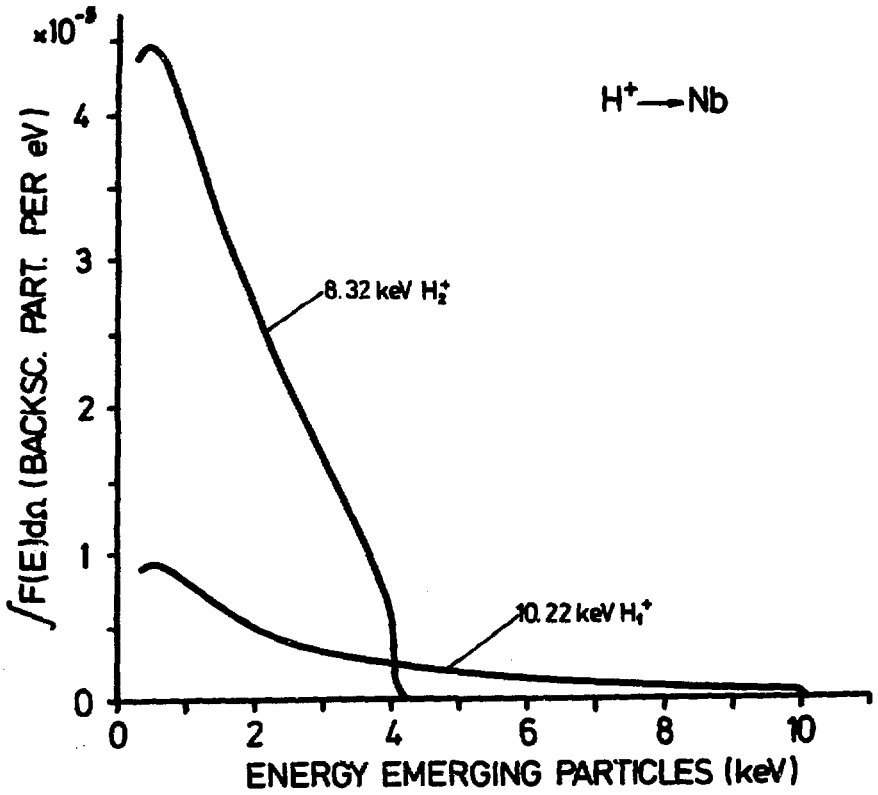
×10⁻⁵
∫F(E)dΩ (BACKSC. PART. PER eV)
H⁺—Nb
8.32 keV H₂⁺
10.22 keV H₁⁺
0
1
2
3
4
0
2
4
6
8
10
ENERGY EMERGING PARTICLES (keV)

Fig. 8

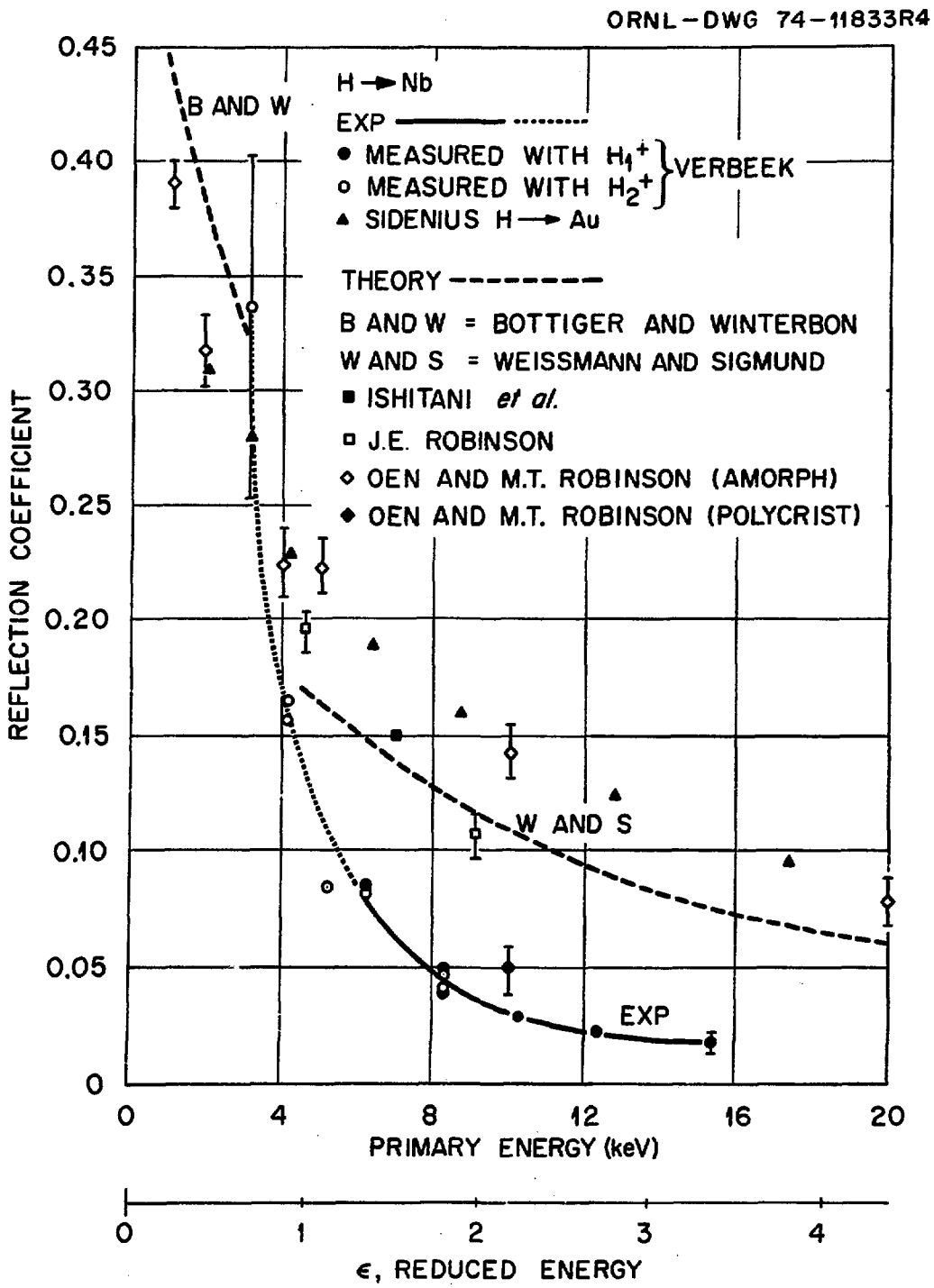
ORNL-DWG 74-11833R4
H → Nb
EXP
MEASURED WITH H_1^+
MEASURED WITH H_2^+
VERBEEK
SIDENIUS H → Au
THEORY
B AND W = BOTTIGER AND WINTERBON
W AND S = WEISSMANN AND SIGMUND
ISHITANI et al.
J.E. ROBINSON
OEN AND M.T. ROBINSON (AMORPH)
OEN AND M.T. ROBINSON (POLYCRIST)
B AND W
W AND S
EXP
REFLECTION COEFFICIENT
0.45
0.40
0.35
0.30
0.25
0.20
0.15
0.10
0.05
0
0
4
8
12
16
20
PRIMARY ENERGY (keV)
0
1
2
3
4
ϵ, REDUCED ENERGY

Fig. 9

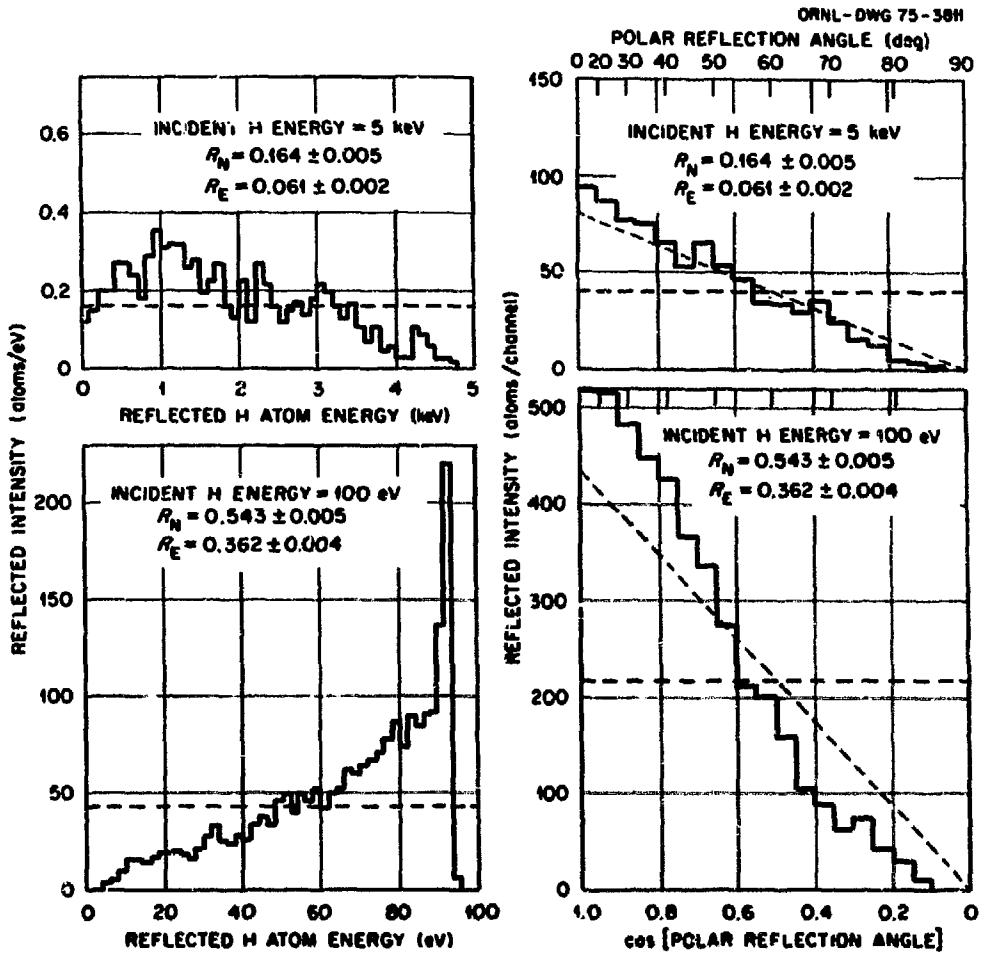

Reflection of H from Amorphous Copper.

Fig. 10